Original Research Article

J. Funct. Mater. Biomol. 1 (2017) 45–50

SACRED HEART RESEARCH PUBLICATIONS

Journal of Functional Materials and Biomolecules

Journal homepage: www.shcpub.edu.in

ISSN: XXXX-XXXX

Investigations on the Effect of Reaction Time on SnS Nanostructures

Ansel Mely L[1], Annie Vinosha P[1], Mary Jaculine M[2], Arun Jose L[3], Jerome Das S[1,*]

Received on 18 Jan 2017, Accepted on 08 Mar 2017

Abstract

As a promising and captivating member of the sulphide family, tin monosulphide (SnS) with its excellent versatility, having fascinating applications with favourable direct and indirect bandgaps, enhanced absorption coefficient (10^5 cm^{-1}), etc., has ignited distinctive interest in the research community. Recently, the material has gained incredible attention as solar absorber, near-infrared detector, photocatalysts, in holographic recording, and many more. SnS nanostructures were prepared by a facile and robust hydrothermal method using tin chloride dihydrate and sodium sulphide as source materials. The reaction was carried out at optimum 200 °C for varying reaction times of 6, 12, 18 and 24 h. The as-synthesized nanostructures were characterized by podwer X-ray diffraction (XRD), High resolution transmission electron microscopy (HR-TEM), Selected area electron diffraction (SAED), UV-visible absorption spectroscopy (UV), Photoluminescence spectroscopy (PL) and dielectric analysis. The XRD and SAED patterns expose the single crystalline nature of the SnS nanostructures. The average particle size calculated by Scherrer equation was found to vary from 15-35 nm for the SnS samples. The effect of the reaction time on the properties of the synthesized nanostructures have been critically evaluated. The optical properties studied by UV and PL advocate that the SnS nanostructures can be pertinent entrants for energy applications.

Keywords: Tin sulphide, Nanostructures, Hydrothermal, Optical properties

1 Introduction

The current era of energy crisis has pushed the scientific commune to find suitable remedy inorder to encounter innovative methods of quenching the energy thirst of the world. Efficient energy materials with low dimensional structures, i.e., nanomaterials, bargain additional attention because of the elevated benefits they provide when paralleled to its bulk counterparts. This added merit is due to their extraordinary surface reactivity and quantum size confinement effects [1,2]. Metal sulphides have become the hub of scientific investigation by material scientists since they have distinctive properties like ample electrical conductivity, cost efficacy, profusion of raw materials, significant catalytic activity, etc., Metal sulphides unveil voluminous merits such as luminescent materials, high-energy density batteries, diagnostic materials, solar energy materials, superconductors, materials for photoelectrolysis and other magnetic applications [3].

Owing to its bewildering properties, metal tin and its compounds are used in many modern and conventional industrial processes like lithography, alloys for electronic circuits, anti-corrosision coating agents and dopants for modern solar cells [4]. Among the metal chalcogenide semiconducting nanoparticles, tin sulphide, with its captivating assets, has gripped researchers to ascertain ways to tune its properties according to the requisite. SnS exhibits exceptional quality of polymorphism and polytypism. Tin sulphide displays a diversity of phases such as SnS_2, SnS, Sn_2S_3, Sn_4S_5 and Sn_3S_4 which can be accredited to the versatile coordinating capacity of tin and sulfur [4, 5]. SnS fits into the category of IV–VI semiconductor and is seen to have a narrow band gap. The material exhibits an orthorhombic structure with herzenbergite modification. The structure if SnSis analogous to that of black phosphorus and possesses a layered structure that consists of six- membered rings. Moreover SnS displays a sturdily distorted NaCl structure. Each tin atom of the SnS unit cell is coordinated by six sulfur atoms in an exceedingly distorted octahedral geometry. The orthorhombic unit cells of the SnS nanocrystal is a compilation of double layers of firmly bound Sn–S atoms. This secure bond that subsists between the layers is of the van der Waals type[6,7]. SnS also exhibits amphoteric nature as they can exist as both p-type and n-type semiconductor depending upon the fabrication conditions with the hole densities of p-type SnS lying in the range of 10^{15}–10^{18} cm^{-3} [8,9].

SnS has a direct band gap of 1.3 eV and an indirect band gap of 1–1.3 eV which are ideal for incredible solar energy conversion [7, 10]. Thin films of tin sulphide demonstrate a fabulous power conversion efficiency of up to 25 % in photovoltaic devices. This is similar to the efficiencies of

* Corresponding author: E-mail: jeromedas.s@gmail.com, jerome@loyolacollege.edu

[1] Department of Physics, Loyola College, Chennai, India - 600 034.

[2] Department of Physics, Velammal Engineering College, Chennai, India – 600 066.

[3] Department of Physics, St. Xavier's College, Palayamkottai, Tirunelveli, India- 627 002.

silicon thin films [11]. The excessive electro negativity and sturdy polarizability of sulfur atoms campaign the active application of tin sulphide as anode material in Li-ion batteries [12]. SnS can also be used as photocalatysts for dye degradation [13], supercapacitors [14], gas sensors [15], optoelectronic material [16], etc. SnS nanoparticles can be meritoriously prepared by various synthesis techniques such as, hydrothermal [17], wet chemical route [18], microwave hydrothermal synthesis [19], solution – dispersion method [20], etc., where hydrothermal method of nanoparticle production is most desirable because of the spectrum of splendid advantages it offers such as better crystallinity, superior nucleation control, prevention of contamination, high purity, enhanced shape control, fine particle size distribution, controlled physical and chemical features. It is noteworthy to mention that the band gap and particle size can be efficaciously tuned depending on the method of synthesis [21]. SnS can be structured into diverse morphologies such as nanorods [2], nanowires [22], nanoflowers [23], nanosheets [24], etc., The present work explicates the ardent fabrication of SnS nanostructures by facile traditional hydrothermal technique using tin chloride dihydrate and sodium sulphide. The absorbing properties of the synthesized nanostructures were investigated and the consequence of reaction time on the structural and optical properties of the nanostructures were assessed.

2 Experimental

2.1 Materials used

The raw materials [tin chloride dihydrate ($SnCl_2.2H_2O$) and sodium sulphide (Na_2S)] were purchased from Sigma Aldrich and used as such for the synthesis. Double distilled water was chosen as solvent for the process.

2.2 Synthesis procedure

Tin monosulphide (SnS) nanoparticles were prepared by a simple and traditional hydrothermal route. Appropriate amount of the precursors were dissolved in 80 ml of distilled water and stirred continuously with the aid of magnetic stirrer to obtain homogeneous solutions. The molar ratio was fixed as 1:3. Sodium sulphide solution was added dropwise into the tin chloride solution and stirred vigorously for 1h at ambient room temperature (303 K). The solution was then emptied into a Teflon-lined stainless steel autoclave of 200 ml capacity and enough care was taken so that the autoclave was filled upto 70% of its volume. It was then firmly sealed and placed in a muffle furnace for 6 h at 200 ^{0}C. This springs way for the production of SnS nanoparticles as the tin ions from tin chloride dihydrate solution and sulphur ions from sodium sulphide solution react. After 6 h the autoclave was removed from the furnace and allowed to cool down to room temperature. The precipitate was washed by multiple centrifugation at 7000 rpm by rinsing sequentially with double distilled water and ethanol to remove the impurities if any. The hence obtained product was dried at 80 ^{0}C overnight to obtain gray solids. On grinding, SnS nanoparticles were obtained. The ground samples were subjected to ultrasonification for 1 h. The experiment was repeated many times by varying the reaction times to 12, 18 and 24 h respectively until the results are consistent. The experimental procedure is exemplified schematically in fig. 1.

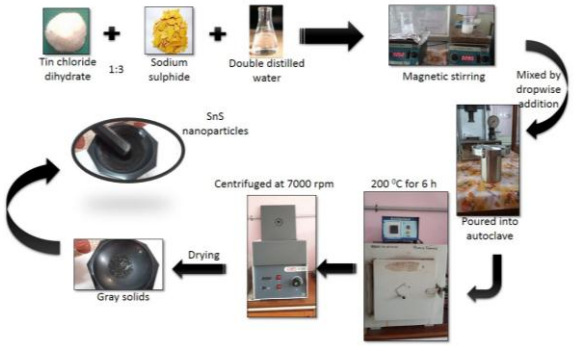

Fig. 1 Schematic representation of the synthesis of SnS nanoparticles

2.3 Mechanism of nanorod formation

Appropriate stoichiometric amounts of the precursors used allow the Sn^{2+} ions and S^{2-} ions to react inside the reaction chamber to form SnS nanoparticles. A schematic depiction of the chemical reaction that takes place is given in fig. 2.

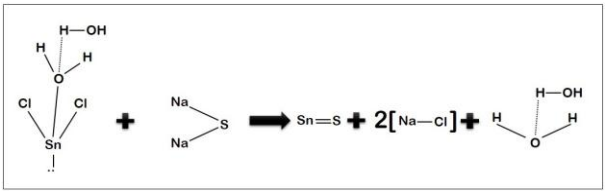

Fig. 2 Chemical equation of formation of SnS nanoparticles

The morphology of the nanoparticle formed depends on the reaction conditions and the nature of the tin atoms in the SnS. The tin atom exists in the 2^+ oxidation state and consequently has an inert lone pair which is in the 5s orbital. This is a vital factor in deciding the nature of crystal growth. The lone pair of electrons stay sterically active and play a significant role in the structure of the SnS. They are responsible for the distortion in the normal rock salt structure thus giving SnS a strong distorted NaCl structure with octahedral geometry which can be attributed to the steric effect [2].

At the required reaction conditions, the lone pair of electrons in the 5s orbital forces the crystal to grow in an elongated (100) direction subsequently forcing the successive layers between the two SnS molecules along the a-axis. In the current work, a reaction temperature of 200 ^{0}C had been applied for various reaction times of 6, 12, 18 and 24 h which leads to the formation varied nanostructures. This growth is attributable to the inert lone pair effect of the Sn (II). The possible mechanism of nanorod formation is represented schematically in fig. 3.

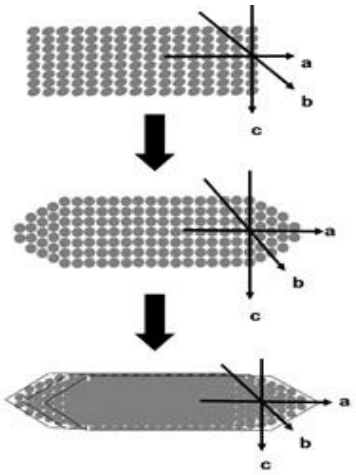

Fig. 3. Schematic representation of possible mechanism of SnS nanorod formation

3 Results and Discussion

3.1 Structural and Morphological Analysis

Fig. 4 shows the XRD diffractograms of SnS nanoparticles amalgamated by hydrothermal technique at varying reaction temperatures. The powder X-ray diffraction analysis was carried out using Bruker AXS D8 Advance instrument with CuKα radiation (λ=1.5406 Å) in the 2θ range 20-70°. It is evident from the multiple intense and distinguishable peaks that the SnS samples were well-crystallized. All the diffraction peaks were agreeable with the standard JCPDS card no. 39-0354.[5] Also the formation of phase pure SnS can be confirmed from the absence of characteristic peaks of impurities such as SnS_2,SnO_2 and metal tin. All the SnS nanoparticles formed by the varying reaction times can be indexed to pure orthorhombic phase herzenbergite, SnS with space group *Pnma.* The crystallite size and lattice strain of the SnS nanopowders can be evaluated by utilizing the peak broadening factor. The corrected peak broadening **(** β)[25] can be derived from the equation

$$\beta = \left[\beta^2_{measured} - \beta^2_{instrumental} \right]^{\frac{1}{2}} \qquad (1)$$

The average crystallite size (D) of the samples were assessed using Scherrer equation[26]

$$D = \frac{k\lambda}{\beta \cos\theta} \qquad (2)$$

Where k is the shape factor equal to 0.89, λ is the wavelength of C_uK_α having the value 1.5406 Å, is the Bragg's angle of the (hkl) reflection given in degrees and β is the full width half maximum (FWHM in radians). Corresponding to the major diffraction peak, the crystallite sizes were found to be 32.64, 30.23, 15.87 and 15.12 nm respectively for the samples synthesized at 6, 12, 18and 24 h. The strain (ε) in the SnS nanostructures which is caused due to the distortion and imperfection in the crystal structure was estimated from the relation, [25]

$$\varepsilon = \frac{\beta}{4\tan\theta} \qquad (3)$$

The interplanar distance (d) of the samples were calculated using the Bragg's equation [27],

$$2d\sin\theta = n\lambda \qquad (4)$$

$$\frac{1}{d^2} = \frac{4\sin^2\theta}{\lambda^2} \qquad (5)$$

which are comparable to the reported results. [5] The dislocation density (δ) was estimated from the formula,[28]

$$\delta = \frac{1}{D^2} \qquad (6)$$

And the results are tabulated in table 1. It is evident from fig. 5, the crystallite size decreases with the increasing reaction time and the lattice strain increases with decreasing crystallite size.

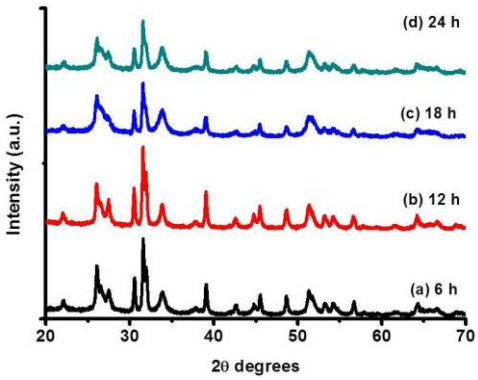

Fig. 4 XRD diffractogram of the synthesized SnS nanoparticles

Table - 1. Some parameters calculated from XRD diffractograms

Reaction time (h)	Crystallite size (nm)	Lattice strain	Dislocation density (nm^{-1})	Interplanar distance (Å)
6	32.64	0.2335	0.00093	2.8293
12	30.23	0.2525	0.00109	2.8334
18	15.87	0.4808	0.00397	2.8324
24	15.12	0.5047	0.00437	2.8324

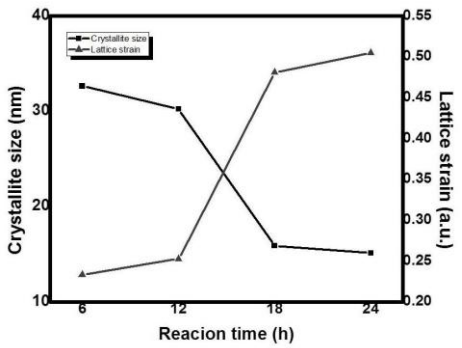

Fig.5. Variation of crystallite size and lattice strain with reaction time Å

HR-TEM analysis was performed to further study the structure and morphology of the primed SnS nanostructures using Joel/JEM 2100 Transmission Electron Microscope. The micrographs presented in fig. 6

(a-d) reveal the formation of nanorod like structures. The SAED pattern given as inset in the corresponding figures can be indexed to orthorhombic structure. It can be seen that the reaction time of 6 h has yielded the formation of nanorod like structures (fig. 6.a).

The size of the nanorods are found to decrease with the increase in reaction time from 6 to 12 h (fig. 6.b). Increased homogeneity is observed when moving from 6 to 12 h. When moving further to 18 and 24 h, a transition from nanorod to nanosheet like structures is manifested (fig.7. c and d). The micrograph in fig. 6.c manifests the distortion of rod to sheet like structure. Also it is obvious that the nanosheets formed at reaction time of 24 h is comparatively larger. The obtained results are similar to that reported in literature[5].The figure 6. e and f clearly depicts the high crystalline nature of SnS nanoparticles. From the obtained results it is evident that the morphology of the final product can be tailored by concentrating on two main factors, *viz.,* the initial nucleation condition of crystal growth and the vapour pressure of the solvents[5]. Herein the reaction time maintained for the hydrothermal synthesis of the SnS nanoparticles was varied which played a crucial role in the morphology of the nanoparticles formed.

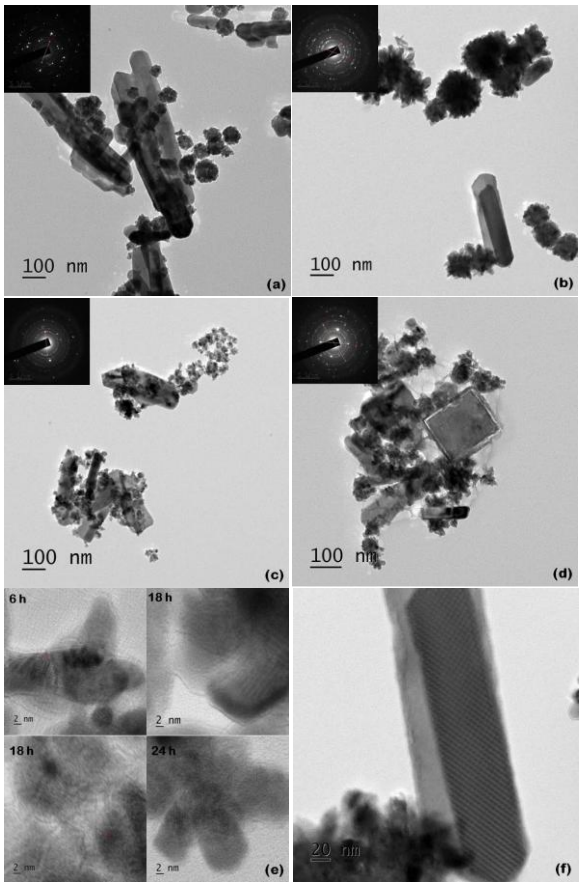

Fig.6. HR-TEM micrographs of the synthesized SnS nanoparticles at different reaction times (a) 6 h (b) 12 h (c)18 h (d) 24 h with inset of corresponding SAED pattern (e) HR-TEM micrographs lattice fringes for the SnS samples (f) nanorod synthesized at 12 h

3.2 Optical Characterization

The optical analysis of the synthesized SnS nanoparticles were carried out using Uv-visible absorption spectroscopy and photoluminescence spectroscopy. The Uv-visible absorption analysis (UV) of the aliquots were carried out using VARIAN in the wavelength range of 500 – 1100 nm. The UV measurements advocate that the developed nanoparticles have an extensive absorption in the visible light expanse. Fig.7. (a-d) shows the Uv-vis absorption spectra of the SnS nanoparticles amalgamated at different reaction times with their corresponding band gap plot of $(\alpha h\nu)^2$ versus photon energy ($h\nu$) as inset. The optimal direct band gap of the SnS nanoparticles, which is an estimate of the corresponding transition of electrons to the conduction band from the valence band, were appraised using the Tauc's law [26]

$$(\alpha h\nu)^n = B(h\nu - E_g) \qquad (7)$$

where α is the absorption coefficient, hν is the energy of photon, B is the proportionality constant and E_g is the direct band gap where n depends on the type of transition. For a direct transition n takes up the value 2. The band gap can be deduced by plotting the curve of $(\alpha h\nu)^2$ vs $h\nu$ and extrapolating the linear part of the curve. The x-intercept of the plot provides the band gap of the nanoparticles. From the corresponding Tauc plots, the band gap of the samples synthesized at reaction time of 6, 12, 18 and 24 h were found to be 1.47, 1.48, 1.50 and 1.51 eV respectively. The obtained band gap falls in the optimal range for solar cell applications and thus the produced SnS nanoparticles can be well suited for energy applications.

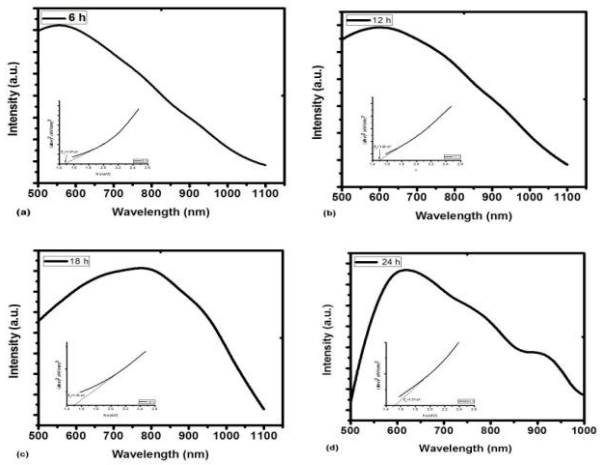

Fig. 7. UV-vis absorption spectra of SnS nanoparticles with inset corresponding plot of $(\alpha h\nu)^2$ versus photon energy ($h\nu$) for different reaction times of (a) 6 h (b) 12 h (c) 18 h (d) 24 h

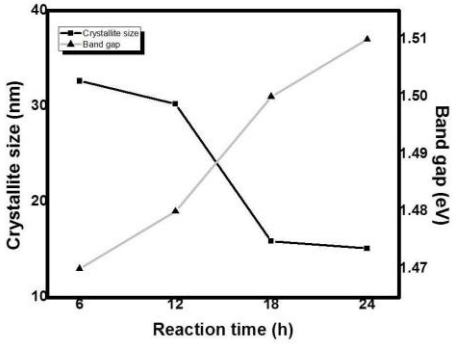

Fig.8. Variation of Crystallite size and band gap with reaction time

Fig. 8 represents the variation of crystallite size and band gap with reaction time. The crystallite size decreases with increasing reaction time and subsequently the band gap increases with the decreasing crystallite size. This is a result of the quantum confinement effects.

Moreover, the Bohr's radius a_B of the SnS nanoparticles has been calculated using the relation

$$a_B = \frac{\varepsilon \hbar^2}{\mu_o e^2} \qquad (8)$$

where ε is the dielectric constant of tin sulphide (fig. 9), $\hbar$ is the reduced Planck's constant which takes the value 1.0545 x 10^{-34} J s, e is the charge of an electron which is equal to 1.6 x 10^{-19} coulomb, and μ_o is the reduced mass of an exciton which is given by

$$\mu_o = \frac{m_e * m_h}{m_e + m_h} \qquad (9)$$

Where, m_e=0.20m_o is the effective mass of an electron in SnS, m_h= 0.36m_o is the effective mass of a hole in SnS and m_o= 9.10938 x 10^{-31} kg is the mass of an electron. The Bohr's radius is estimated to be 7.12, 6.91, 6.80 and 6.53 nm for the SnS samples prepared at 6, 12, 18 and 24 h respectively. It could be perceived that only weak confinement of electrons is possible since the estimated Bohr's radius is lower than the diameter and length of the SnS nanorods obtained [2].

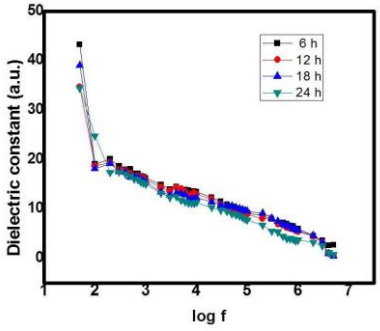

Fig. 9. Variation of log f vs dielectric constant for the SnS nanoparticles

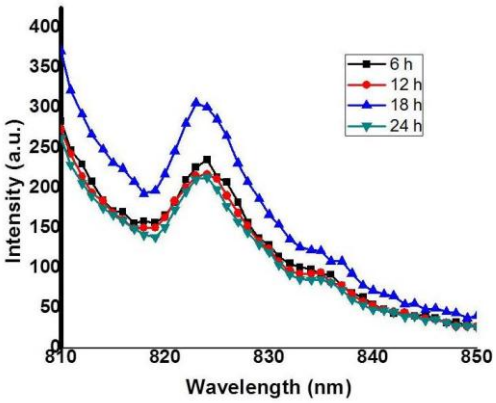

Fig. 10. Photoluminescence spectra of the synthesized SnS nanostructures

Fig.10 represents the Photoluminescence (PL) spectra of the hydrothermally synthesized SnS nanostructures recorded at room temperature. It is apparent from the graph that all the four samples display a strong emission around 823 nm. Thus we can observe a red shift in the spectra. The detected emission peak is dissimilar to that of SnS_2 (570 nm) and bulk SnO_2 (360 nm) [29]. This identified emission can be well attributed to prominent transition in the hydrothermally prepared SnS semiconductor nanostructures.

4 Conclusions

Tin monosulphide (SnS) nanoparticles were effectively synthesized by a simple, effective and traditional hydrothermal route by varying the time of the samples in the reaction chamber for a fixed temperature of 200 °C. The synthesis was carried out for 6, 12, 18 and 24 h. The average size of the nanoparticles formed were in the range of 15-35 nm. The XRD patterns revealed the formation of excellent and orthorhombic phase herzenbergite, SnS with space group *Pnma*. The HR-TEM studies divulged the formation of nanorod like structures which gradually moved on to sheet like structures with the increasing reaction times. The optical analysis reveal the fact that the PL emission has had a red shift. The direct optical band gap estimated from the Tauc plot were found to vary from 1.47-1.51 eV. The synthesized nanoparticles exhibited a decrease in crystallite size with increasing reaction times whereas the band gap increased. It is evident that the obtained SnS nanoparticles with its astounding properties can be employed for energy applications.

Acknowledgements

One of the authors (SJD) is grateful to the management of Loyola College, Chennai - 34 for awarding the project (3LCTOI14PHY002) through which some required facilities for the synthesis of materials were fabricated and the technical support by the SAIF-STIC, Cochin and Department of Chemistry, Ethiraj College for Women, Chennai are gratefully acknowledged.

References

[1] Jun Liu, DongfengXue, *Electrochim. Acta*, 56, (2010) 243.

[2] Alok M. Tripathi, SagarMitra, *RSC Adv.,* 4, (2014) 10358.

[3] P. Balaz, L. Takacs, T. Ohtani, D.E. Mack, E. Boldizarova, V. Soika, M. Achimovicova, *J. Alloys Compd.,* 337, (2002) 76.

[4] Jitender Gaur, Shilpa Jain, Suresh Chand, Narendra Kumar Kaushik, *Am. J. Anal. Chem.,* 5, (2014) 50.

[5] Subhajit Biswas, SoumitraKar, Subhadra Chaudhuri, *Appl. Surf. Sci.,* 253, (2007) 9259.

[6] K.G. Deepa, J. Nagaraju, *Mater. Sci. Eng., B,* 177, (2012) 1023.

[7] WangshengGao, Chuangsheng Wu, Meng Cao, Jian Huang, Linjun Wang, YueShen, *J. Alloys Compd.,* 688, (2016) 668.

[8] Yashika Gupta, P. Arun, A. A. Naudi, M. V. Walz, E. A. Albanesi*, Thin Solid Films,*612, (2016) 310.

[9] Fan-Yong Ran, Zewen Xiao, Yoshitake Toda, HidenoriHiramatsu, Hideo Hosono, Toshio Kamiya, *Sci. Rep*., 5, (2015) 10428.

[10] Zhijie Wang, Shengchun Qu, Xiangbo Zeng, Junpeng Liu, Furui Tan, Yu Bi, Zhanguo Wang, *Acta Mater.,* 58, (2010) 4950.

[11] Xing-Long Gou, Jun Chen, Pan-Wen Shen, *Mater. Chem. Phys.,* 93, 557 (2005)

[12] Y. Li, J.P. Tu, X.H. Huang, H.M. Wu, Y.F. Yuan, *Electrochem. Commun.,* 9, (2007) 49.

[13] Peisong Tang, Haifeng Chen, Feng Cao, Guoxiang Pan, Kunyan Wang, Minghong Xu, Yanhua Tong, *Mater.Lett.,* 65, (2011) 450.

[14] Yang Li, HuaqingXie, JiangpingTu, *Mater. Lett.,* 63, (2009) 1785.

[15] Hassan Karami, SomayyehBabaei, *Int.J. Electrochem. Sci.,* 8, (2013) 12078.

[16] S. F. Wang, W. Wang, W. K. Fong, Y. Yu, C. Surya, *Sci. Rep*., 7, (2017) 39704.

[17] Masoud Salavati-Niasari, Davood Ghanbari, Fatemeh Davar, *J. Alloys Compd.,* 492, (2010) 570.

[18] S. Sohila, M. Rajalakshmi, Chanchal Ghosh, A.K. Arora, C. Muthamizhchelvan*, J. Alloys Compd.,* 509, (2011) 5843.

[19] Xinlong Yan, Elizebeth Michael, Sridhar Komarneni, Jeffrey R. Brownson, Zi-Feng Yan, *Ceram. Int.,* 39, (2013) 4757.

[20] Yanbao Zhao, Zhijun Zhang, Hongxin Dang, Weimin Liu, *Mater. Sci. Eng., B*, 113, (2004) 175.

[21] K. Byrappa, T. Adschiri, Progress in Crystal Growth and characterization of Materials, 53, (2007) 117.

[22] Yingkai Liu, DedongHou, Guanghou Wang, *Chem. Phys. Lett.,* 379, (2003) 67.

[23] Hongliang Zhu, Deren Yang, Hui Zhang, *Mater. Lett.,* 60, (2006) 2686.

[24] S. Sohila, M. Rajalakshmi, C. Muthamizhchelvan, S. Kalavathi, Chanchal Ghosh, R. Divakar, C.N. Venkiteswaran, N.G. Muralidharan, A.K. Arora, E. Mohandas, *Mater. Lett.,* 65, (2011) 1148.

[25] V. D. Mote, Y. Purushotham, B.N. Dole, *Journal of Theretical and Applied Physics,* 6, (2012) 6

[26] Annie Vinosha P, AnselMely L, EmimaJeronsia J,Krishnan S, Jerome Das S, *Optik*, 10.1016/j.ijleo.2017.01.018

[27] R. Udayakumar, V. Khanaa, T. Saravanan, *Indian J. Sci. Technol*., 6 (6s), (2013) 4754.

[28] S Velumani, Sa K Narayandass, D Mangalaraj, *Semicond. Sci. Technol.,* 13, (1998) 1016.

[29] Ghosh B, Das M, Banerjee P, Das S, *Semicond. Sci. Technol.,* 23, 1 (2008) 125013.